DECAMETER-SCALE MORPHOLOGIC AND STRUCTURAL MARTIAN MAPPING OF LAYERED BEDROCK IN CRATER CENTRAL UPLIFTS. A. M. Nuhn[1], L. L. Tornabene[1,2], G. R. Osinski[1], and A. S. McEwen[3]. [1]Centre for Planetary Science and Exploration, Western University, London, ON, N6A 5B7 Canada (anuhn4@uwo.ca), [2]SETI Institute, Mountain View, CA 94043, USA, [3]Lunar and Planetary Laboratory, University of Arizona, Tucson Arizona, USA.

Introduction: Central uplifts within complex impact craters expose faulted, rotated, and deformed deeply-seated bedrock from the subsurface and thus provides important insights with respect to the subsurface geology and the formation of central uplifts [1,2,3]. Layered central uplifts are very useful in structural geologic studies as the orientations of their layers provide a frame of reference (i.e., the folding, faulting, and rotation of layers) that can be used to decipher the deformation history of the central uplift [2,4]. Despite their importance for understaning planetary crusts, much remains unknown about the detailed mechanics of central uplift formation, including weakening mechanisms and the exact depth of origin of exposed lithologies in the pre-impact target.

In this study, three complex craters with central uplifts containing layered bedrock morphologies were selected for detailed mapping. The craters are all ~30 km in diameter, contain well-exposed bedrock, and are located in regions known for prolonged history of effusive volcanic activity that have produced voluminous layered, cyclic volcanic deposits that were likely flat-lying and relatively undisturbed prior to impact [5]. Morphologic and structural mapping using high-resolution images of these layered crater central uplifts may provide the best constraints on the structural history, and thereby, the mechanisms involved in the formation of central uplifts. We set out to compare and contrast the deformed layered bedrock within the central uplifts of these complex craters of a similar size to place constraints on current uplift models [6] and better understand central uplift formation in mid-sized complex craters. Here we present our preliminary morphologic and structural mapping of three unnamed Martian craters.

Background: The three craters of this study were selected from the Crater-Exposed Bedrock (CEB) database complied by Tornabene et al. [7]. The first unnamed crater is located in the Solis Planum Region (281° E, 4° N) with a diameter of ~31 km. The central uplift in this crater has a diameter of ~9 km and displays a pit morphology (Fig. 1a). The second unnamed crater is located in the Noachis Terra Region (304° E, 26° S) with a diameter of ~31km. The central uplift in this crater has a diameter of ~11km and peak-pit morphology (Fig. 1b). The last unnamed crater is located in Thaumasia Planum (294° E, 26° 6) and has a ~27 km-diameter with a peak-pit ~6 km in diameter (Fig. 1c).

Layered Bedrock: The layered bedrock in these three uplifts have a consistent and distinctive appearance. Darker-toned, lava layers are observed to alternate with lower-standing, weaker, light-toned sedimentary or volcanogenic (possibly ash) layers [8]. Approximately 90% of all crater-exposed layered bedrock occur in Hesperian volcanic plains units [2]. Hesperian ridged plains have been mapped [9] over widespread regions of Mars and have been interpreted to be volcanic flood lavas [10].

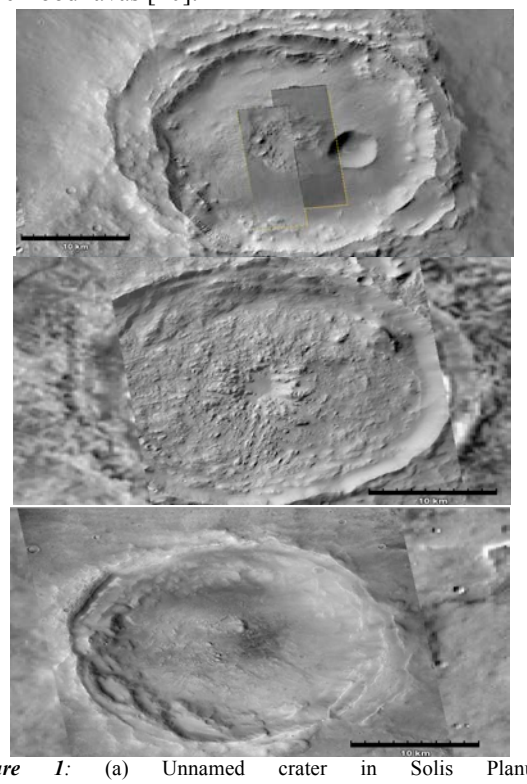

Figure 1: (a) Unnamed crater in Solis Planum (ESP_016805_1565_RED.JP2 and ESP_027987_1565_RED.JP2). (b) Unnamed crater in Noachis Terra (B19_017002_1538_XN_26S056W). (c) Unnamed crater is Thaumasia Planum (G09_021578_1541_XN_25066W). Image credit: NASA/JPL/MSSSS/ASU/UA/JMARS.

Data Required: Images from the High Resolution Imaging Science Experiment (HiRISE) onboard the Mars Reconnaissance Orbiter (MRO) provides images with resolutions as high as ~0.25 m/pixel [11]. Only HiRISE data can resolve the small-scale features on central uplifts that allow detailed structural and morphological mapping. Non-orthorectified HiRISE images are currently used as our base map and will be compared with orthorectified images in future work. Our base map is supported by various other data products including, Mars Orbiter Laser Altimetry (MOLA) data [12]; both visible and thermal infrared images (including thermal inertia) from the Thermal Emission Imag

ing System (THEMIS) [13], context camera (CTX) images [14], High-resolution DTMs (HiRISE and HRSC) [11] and a few selected spectral parameter images derived from hyperspectral data from the Compact Reconnaissance Imaging Spectrometer for Mars (CRISM) [15].

Mapping Methods: ESRI ArcGIS and JMARS software are used to map the three craters in our study. Geological units are mapped by correlating similar unit characteristics on the central uplifts using the various datasets. Mapping of structural features including, dykes, faults, and layer orientations, as well as overprinting primary and secondary impacts are also underway.

Results: The following geologic units are based on morphologic, textural, and structural characteristics of the central uplifts. Letters indicate corresponding unit on the geologic map (Fig. 2).

Aeolian Deposits (A). This unit contains accumulations of sand-sized materials transported through saltation with consistent Aeolian bedforms as observed elsewhere on Mars and on Earth. These deposits are typically found in lower elevations/depressions as well as flat terrains within the central uplift.

Undifferentiated Deposits (U). This unit is comprised of a uniform, likely fine-grained, materials that overlie much of the central uplift.

Layered Bedrock (LBr). Layered Bedrock is divided into interbedded with lighter darker- and lighter-toned layers as observed by Tornabene et al. [7]. The layers are reported to have a strong olivine spectral signatures in CRISM data [3]. This unit has multiple exposures of bedrock in these central uplifts. The bedrock appears to have been fractured, folded and faulted, which likely occurred during crater formation [2].

Impact Melt (IM). This relatively dark-toned unit has a very smooth texture with little to a great deal of preserved overprinting craters and other characteristics consistent with the description in Marzo et al. [16]. It is located throughout the central uplift as well as the crater floor.

Shadow (S). This unit is consistent with heavily shadowed areas in the HiRISE RED mosaic images. Shadows occur depending on the solar azimuth and viewing angles when the image was taken.

Rough (R). This unit consists of coarsely-textured highly eroded rock.

Sculpted (Sc). This unit has a scalloped texture typically occurring just beneath the edge of topographic highs in the central uplift. This unit is thought to occur due to wind erosion.

Regolith (Re). This unit includes unconsolidated materials, including soils, dust, and boulders.

Future work: Once mapping is complete for all three craters, structural and morphological features in layered, megabreccia, and fractured bedrock in Martian impact crater central uplifts will be identified, compared and contrasted. DTMs will be used to produce balanced cross-sections and interpretion of the structures. Understanding similarities and differences between the three craters may potentially answer questions such as: what effects do target lithologies play in central uplift formation and bedrock morphologies? And, what role might dykes have played in the formation of central uplifts? Future work in this study will involve mapping other craters with central uplift bedrock morphologies that include, megabreccia and massive-fractured types [7].

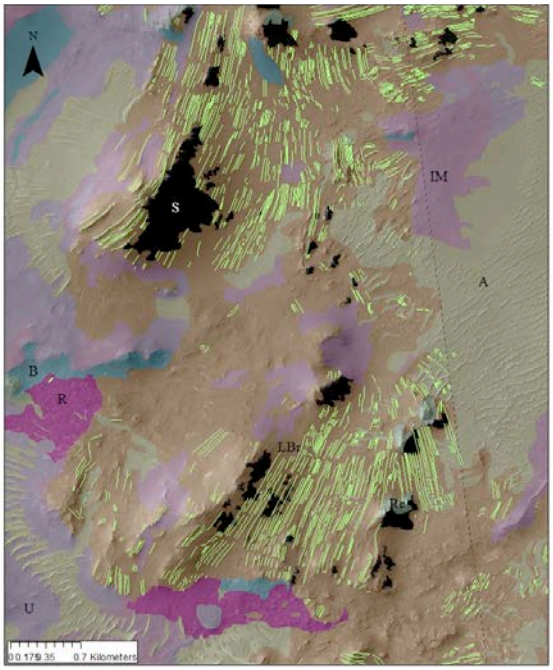

Figure 2: Digitized unit map from ArcMap of the western portion of the Unamed Crater in Solis Planum. Yellow lines mark tilted bedrock layers.

References: [1] Tornabene et al. (2012) *3rd Early Mars abstract*. [2] Caludill et al. (2012) *Icarus*, 221, 710-720. [3] Quantin C. et al., (2012) Icarus 221, 436-452. [4] Wulf et al., 2012, Icarus 220, 194-204, terrestrial crater studies. [5] Nichols R. L. (1936) *J. Geol., 44*, 617-630 [6] Melosh H. J. (1989) *Oxford, Oxford University Press*, p.245. [7] Tornabene L.L. et al. (2010) LPSC XVI, Abstract #1737. [8] Golombek M P. et al. (2001) *JGR, 106*, 23811-23821. [9] Skinner J. A. et al. (2006) LPSC XXXVII, Abstract #2331. [10] Scott D. H. and Tanaka K. L. (1986) *USGS Map I-1802-A*. [11] McEwen et al., (2007) *JGR*, *32*: L21316. [12] Smith D. et al., (2001) *JGR, 106*: 689-722. [13] Christensen, P. R. et al., (2004) *Space Sci. Rev., 110*: 85-130. [14] Malin M. C. et al., (2007) *JGR, 112*: E05S04. [15] Murchie S. et al., (2007) *JGR, 112*: E05S03. [16] Marzo G. A. et al. (2010) Icarus, 208, 667-683.